Magnetotelluric Analysis for Greenland and Postglacial Isostatic Evolution (MAGPIE)

1. Relevance relative to the call for proposals

Scientific Merit and Innovation. Melting of the Greenland Ice Sheet has been accelerating in the past decade as the climate warms [*Harig and Simons*, 2016] and is now considered to be a major contributor to present-day sea level change [*Frederikse et al.*, 2018]. As the ice melts, the rocks beneath the ice become unloaded and rebound elastically, causing surface uplift that can be measured using GPS [*Simpson et al.*, 2011]. In addition, the ground surface of Greenland is also deforming slowly in response to melting that happened during the past ice age [*Wake et al.*, 2016]. This process is called glacial isostatic adjustment (GIA). These two causes of uplift, due to present and past melting, are mingled in modern geodetic observations. The GIA component is difficult to predict because it is sensitive to mantle viscosity, which is largely unconstrained beneath Greenland. Indeed, GIA patterns may be especially complex because Greenland mantle viscosity is likely to vary laterally: much of the Greenland mantle is old and cold and therefore stiff, while the portion beneath central Greenland has been impacted by the Iceland plume and is therefore likely to be hotter and weaker [*Khan et al.*, 2016; *Rogozhina et al.*, 2016]. The impact of these viscosity variations on GIA is untested.

Objective: Constrain present-day melting rates in Greenland by accurately correcting observed uplift rates for glacial isostatic adjustment (GIA) from past deglaciation.
- The Iceland plume likely produced lateral viscosity variations beneath Greenland.
- We will collect magnetotelluric (MT) data to constrain these viscosities.
- We will develop a new GIA model that incorporates these viscosity variations.

In this project we will collect magnetotelluric data across Greenland to measure the electrical properties of the mantle beneath the Greenland Ice Sheet and better constrain its lateral viscosity variations. We will determine whether there is a hot, low-viscosity channel in the mantle beneath central Greenland that was left by the passage of the Iceland plume. By imaging sub-ice melt, we will also test predictions that this plume track promotes sub-ice melting [*Rogozhina et al.*, 2016]. Building on these observations, we will construct a new set of GIA models for mantle flow beneath Greenland that include lateral variations in viscosity. These models will remove significant uncertainty from estimates of present-day ice mass loss in Greenland.

National and International Collaboration. This project involves international collaborations between researchers in Norway with those in Australia, Denmark, Germany, Canada, and the USA, as well as national collaborations between the Universities of Oslo and Bergen. This project will enhance the activities of these researchers and will foster synergistic and interdisciplinary collaboration among them.

Student and Postdoctoral training. We plan to recruit one postdoctoral scholar, one PhD student, and 2-3 Masters students, who will join the Earth Modelling group at CEED under Conrad's supervision. These individuals will receive valuable training while performing MT fieldwork and analysis and geodynamic modelling as part of this interdisciplinary research project. We will advertise these positions internationally to recruit the best applicants, and will prioritize female applicants.

Relevance to Society. By incorporating lateral viscosity variations, we will develop a new class of GIA models that will provide new constraints on ground motion occurring in response to the last major deglaciation. For Greenland, these models will help to constrain patterns of present-day melting, which is a major source of modern-day sea level rise that is critical for coastal areas globally (including Norway). We plan to communicate the results of this project in scientific publications and associated press releases and media outreach. We will also incorporate the discoveries of this project into active learning environments intended for broader outreach, such as those presented at CEED's annual booth at Forskningstorget.

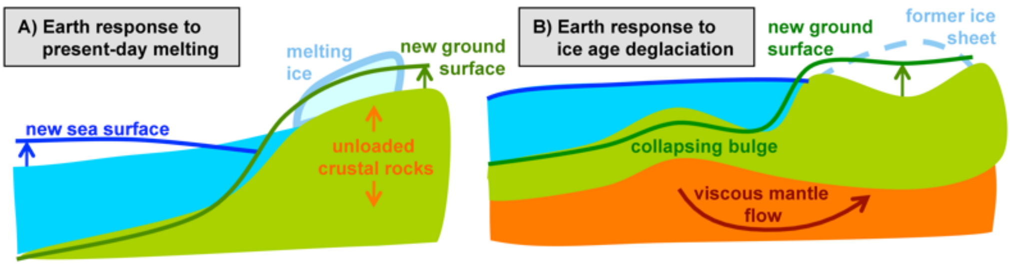

Figure 1. Two mechanisms drive ground motion in Greenland: (A) Climate change-induced melting of the Greenland ice sheet causes unloading of the crust and surface uplift. (B) The ground surface is also responding to deglaciation that occurred 15,000 – 8000 years ago. This glacial isostatic adjustment (GIA) results from mantle flow and is sensitive to mantle viscosity.

2. Aspects relating to the research project

Background and status of knowledge

2.1. Earth structure must be known to monitor ice sheet melting

In order to track and mitigate the effects of climate change, the volume of ice lost from the great continental ice sheets in Antarctica and Greenland must be monitored. The methods employed to do this rely on measurements of gravity and altimetry and consist of (1) satellite measurements of time-variations in gravity (e.g., from the GRACE satellites) [*Luthcke et al.*, 2013]; (2) satellite altimetry that measures changing ice sheet elevation [*Hurkmans et al.*, 2014]; (3) local gravity measurements [*Nielsen et al.*, 2014]; and (4) GPS measurements from stations attached to bedrock surrounding the ice sheets [*Khan et al.*, 2010].

These measurements all rely on the fact that, as ice melts, mass is lost from the ice sheet and the gravitational attraction and elevation of the ice sheet are reduced. If the 'solid Earth' were truly solid and did not deform, it would be trivial to use these measurements to calculate the ice loss. However, such calculations are made much more complex by the fact that the Earth deforms in response to ice sheet mass changes, in two ways:

(1) *Instantaneous elastic deformation*. Earth's rocks deform elastically in response to applied loads. Thus, we expect ground uplift in the vicinity of deglaciation as rocks below the melting ice decompress (Fig. 1a). This deformation occurs instantaneously and constrains the total mass of melting [*Conrad*, 2013].

(2) *Glacial isostatic adjustment (GIA), also referred to as post-glacial rebound (PR)*. The Earth's mantle is viscous and deforms slowly to changes in applied stress. Just as a foam mattress rebounds slowly after someone gets off it, the mantle also rebounds slowly after the mass of an ice sheet is removed by melting. Indeed, the mantle today is still responding to changes in ice sheet mass that occurred thousands of years ago [*Peltier*, 2004]. Typically, this response involves flow from the periphery to the interior of the former ice sheet. These areas experience subsidence and uplift, respectively (Fig. 1b).

Excellent constraints on the structure of the Earth below the ice sheet are vital in order to accurately relate geodetic observations to constraints on present-day mass loss. To demonstrate this, we computed the elastic response of the Earth to recent Greenland melting (Fig. 2a). These models predict uplift of 2-5 mm/yr and faster rates on the periphery of the ice sheet where mass loss rates are faster. However, measurements of this deformation are obscured by the on-going GIA response to past deglaciation. We computed this GIA uplift using two different mantle viscosity structures (Figs. 2b and 2c). We found that the GIA-induced vertical motion is generally larger in magnitude than the elastic deformation (cf. Fig. 2a) and exhibits a complex pattern that depends significantly on mantle viscosity structure. Clearly, mantle viscosity must be constrained to accurately remove GIA deformations from geodetic observations.

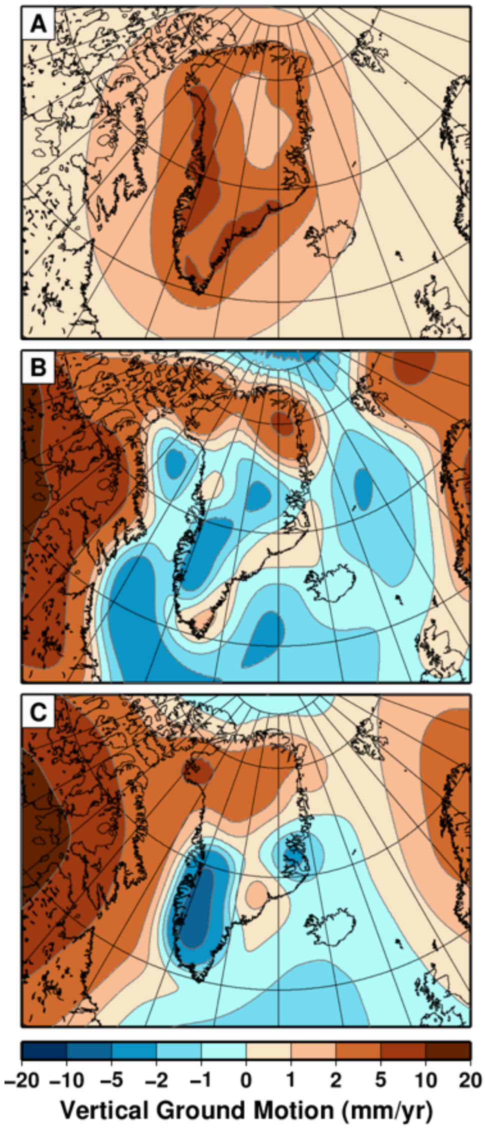

Figure 2. Models of vertical ground motion for the North Atlantic, showing patterns of uplift (red) and subsidence (blue) resulting from:

(a) Earth's elastic response to recent mass loss in Greenland during 2003-2016. We computed the Earth's elastic response following *Conrad* [2013] and applying GRACE-inferred rates of Greenland mass loss, as compiled by *Luthcke et al.* [2013] and updated based on more recent observations.

(b) Earth's ongoing viscous response to past deglaciation, computed here by applying the SELEN sea level solver (which solves for solid earth deformation and sea level assuming a viscoelastic rheology) [*Spada and Stocchi*, 2007] to the ICE-5G ice history model [*Peltier*, 2004]. Here we have assumed a layered mantle viscosity structure consistent with the volume-averaged viscosity profile used by *Peltier* [2004].

(c) Earth's viscous response, but with reduced viscosity for the uppermost mantle. This calculation is identical to that in (b), but the viscosity at 90-420 km depth has been decreased by a factor of 5. This change significantly affects patterns of GIA uplift.

2.2. Mantle viscosity beneath Greenland is currently poorly constrained and likely varies laterally

Currently, the 3D mantle viscosity structure beneath Greenland is poorly known and this deficiency is seriously impacting the quality of ice loss calculations. For instance, *Velicogna* [2009] called the GIA correction 'the largest source of uncertainty in [the] ice mass estimate' in Greenland. In this project, we will produce robust constraints on the laterally-varying mantle viscosity beneath Greenland and develop 3D dynamic models of interactions between Earth deformation, ice sheet behaviour, gravity, and elevation.

Mantle strain rate ($\dot{\varepsilon}$) is controlled by stress (σ), temperature (T), grain size (d), and composition, specifically hydrogen (or water) content, (C_w) and presence of partial melt fraction (φ), as described by

$$\dot{\varepsilon} = A\sigma^n d^{-p} {C_w}^r \exp(\alpha\varphi) \exp\left(\frac{-\Delta H}{RT}\right) \quad \text{(Equation 1)}$$

[e.g., *Hirth and Kohlstedt*, 2003], where A and α are constants, n, p and r are the stress, grain size and water content exponents, ΔH is the activation enthalpy, and R is the gas constant. A complete characterization of mantle viscosity requires all these parameters to be known.

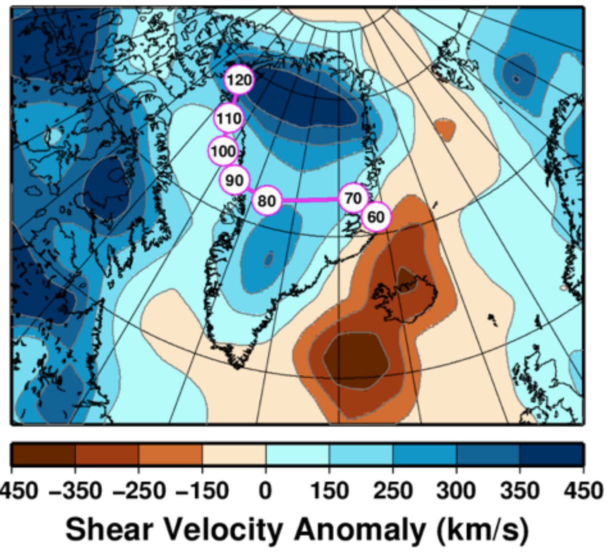

Figure 3. Shear velocity anomalies at 150 km depth beneath the North Atlantic from the *Schaeffer and Lebedev* [2013] tomography model, showing lateral variations beneath Greenland. The postulated track of the Iceland plume (magenta), reconstructed for 120-60 Ma based on [*Doubrovine et al.*, 2012] runs through the region of low shear velocities (assumed higher temperatures), as noted by *Rogozhina et al.* [2016]. The seismic anomalies may be associated with lateral viscosity variations, which should significantly affect the GIA response to past deglaciation [*Khan et al.*, 2016].

The complex geological history of the Greenland lithosphere has produced significant variations in composition and geotherm, and these are likely to be associated with large viscosity heterogeneities. Much of the exposed Greenland basement is Archean to Paleoproterozoic in age, dominated by the Archean Greenland Craton in southern Greenland [e.g., *Windley and Garde*, 2009] and the surrounding Paleoproterozoic and reworked Archean belts [e.g., *Nutman et al.*, 1999]. Paleoproterozoic and reworked Archean rocks have also been found at Victoria Fjord in northernmost Greenland [*Nutman et al.*, 2008] and in the GISP2 drillhole at Summit Station [*Weis et al.*, 1997], suggesting that Archean to Paleoproterozoic lithosphere underlies many parts of Greenland that are covered by ice or younger rocks (see Fig. 6). The lithospheric mantle beneath these domains has been sampled by extensive Precambrian to Mesozoic kimberlite and lamproite volcanism, particularly in south-west and south-east Greenland. These xenoliths show that the Greenland Craton's uppermost mantle has a highly depleted composition, demonstrating incompatible element contents that are low even compared to other Archean cratons [e.g., *Bernstein et al.*, 2006; *Bernstein et al.*, 1998; *Bizzarro and Stevenson*, 2003; *Griffin et al.*, 2009]. Since hydrogen is also an incompatible element, these geochemically depleted compositions would be expected to be associated with low hydrogen contents. Combined with low cratonic geotherms, these compositions would imply high viscosities for the Archean to Paleoproterozoic parts of Greenland (Eq. 1).

The Greenland lithosphere has been impacted by multiple metasomatic events from the Proterozoic to the Phanerozoic, producing changes in mantle composition both laterally and with depth [*Aulbach et al.*, 2018; *Bizzarro and Stevenson*, 2003]. For viscosity, the most important of these events is the postulated passage of Central Greenland over the Iceland plume during the Cretaceous and early Cenozoic. This passage is marked by the eruption of flood basalts on the western Greenland coast from ~64 Ma and on the eastern Greenland coast from ~56 Ma [e.g., *Storey et al.*, 1998; *Tegner et al.*, 2008]. Geological and paleomagnetic data have allowed various authors to reconstruct the plume track as an east-west trending corridor through central Greenland [e.g., *Doubrovine et al.,* 2012; Fig. 3]. The Iceland plume is estimated to be ~165 K hotter than standard mid-ocean ridge mantle [*Putirka*, 2005] and likely contains higher hydrogen contents [*Nichols et al.*, 2002], both of which would lead to low viscosities (Eq. 1). The plume track has also been linked to high surface heat flows and subsequent increased basal melting of the ice cap [*Rogozhina et al.*, 2016]. Seismic tomography models [e.g., *Schaeffer and Lebedev*, 2013] show comparatively slow seismic velocities below the Iceland plume track (Fig. 3), consistent with higher temperatures and more fertile compositions, while the lithospheric mantle beneath southern and northern Greenland displays faster seismic velocities consistent with colder temperatures and more depleted compositions. These factors should result in significant viscosity variations between the low viscosity plume track and the high viscosity surrounding mantle. However, without better constraints on the parameters in Equation 1, the actual viscosities remain poorly constrained.

2.3. Earth models used in Greenland GIA models do not take into account these viscosity structures

Most GIA models assume that the viscosity structure of the upper mantle is laterally homogenous, consisting of several layers of uniform viscosity. This assumption of a radially symmetric structure is made to allow the viscoelastic loading problem to be solved relatively quickly in the spectral domain [*Mitrovica et al.*, 1994]. It also permits direct coupling to solvers for the sea level equation, which account for redistributions of water loads associated with deflections of the land and sea surfaces [*Spada and Stocchi*, 2007]. Incorporation of lateral viscosity variations generally requires more sophisticated and computationally more expensive finite volume [*Latychev et al.*, 2005] or finite element [*Paulson et al.*, 2005] approaches. Initial studies of the impact of lateral viscosity variations on GIA for Antarctica [*van der Wal et al.*, 2015], Fennoscandia [*Whitehouse et al.*, 2006], and Canada [*Paulson et al.*, 2005] show important differences compared to radially-symmetric models. In their recent review into the current state of GIA modelling, *de Boer et al.* [2017] named incorporation of 3D mantle viscosity variations as one of the most important 'future perspectives' for improving GIA models. In particular, these studies suggest that the GIA response for any particular location is sensitive to viscosity structures both locally and beneath the deglaciated region [*Paulson et al.*, 2005].

Greenland has a deglaciation history of its own and it also lies on the peripheral bulges of both the Fennoscandian and Canadian deglaciations. As a result, we expect that Greenland GIA will be influenced by lateral variations in viscosity, especially those associated with the Iceland plume track beneath Greenland itself. Indeed, *Kahn et al.* [2016] observed unusually rapid uplift in southeast Greenland that can be attributed to faster GIA uplift in this area compared to elsewhere in Greenland, but this behaviour is not predicted by current GIA models with layered viscosity structures [*Lecavalier et al.*, 2014]. Low mantle viscosity beneath this area – presumably created since the Cretaceous via the thermal, mechanical [*Steinberger et al.*, 2015] and compositional effects of the Iceland plume (Fig. 3) – could explain the faster uplift rates [*Khan et al.*, 2016], but this idea has not yet been tested by a GIA model that properly accounts for lateral viscosity variations in the uppermost mantle. We propose to develop such models here.

Approaches, hypotheses and choice of method

*2.4. **Hypothesis 1**: MT data can improve estimates of Greenland mantle viscosity*

To improve constraints on Greenland mantle viscosity, we will collect new magnetotelluric (MT) data at locations on the Greenland Ice Sheet both over and distal from the Iceland plume track. MT is one of the most important datasets for constraining viscosity [e.g., *Liu and Hasterok*, 2016; *Selway*, 2015] but currently no MT data exist over the Greenland Ice Sheet. MT is a passive electromagnetic geophysical technique that measures the electrical conductivity of the Earth to upper mantle depths. Due to electrical storms and the impact of the solar wind, Earth's magnetic field is always fluctuating and this induces currents in conductive bodies within the Earth. In the MT method, the fluctuating electric and magnetic fields are measured at stations on the Earth's surface to produce models of the electrical structure of the lithosphere and asthenosphere.

The main variables that control mantle viscosity are temperature, hydrogen content and the presence of partial melt (Eq.1). Importantly, these are also the primary controls on the electrical conductivity of the mantle. The electrical conductivity (σ) of silicate minerals, which constitute the bulk of the mantle, is defined by:

$$\sigma = AC_w^r \exp\left(\frac{-\Delta H}{RT}\right) \quad \text{(Equation 2)}$$

where A is a constant, C_w is the hydrogen (or water) content, ΔH is the activation enthalpy, T is the temperature and R is the gas constant. Since melt is generally significantly more electrically conductive than crystalline minerals [e.g., *Sifré et al.*, 2014], the presence of an interconnected melt phase will also dramatically increase the conductivity of the mantle. A comparison between Equations 1 and 2 shows the strong correspondence between electrical conductivity and strain rate (e.g., Fig. 4). This is because both deformation and electrical conduction rely on the movement of particles. The bulk mantle minerals are nominally anhydrous, so the presence of hydrogen ions as point defects dramatically enhances diffusion due to their tiny particle size. Temperature also increases both strain rate and conductivity since particles have more energy to move at higher temperatures (Fig. 4).

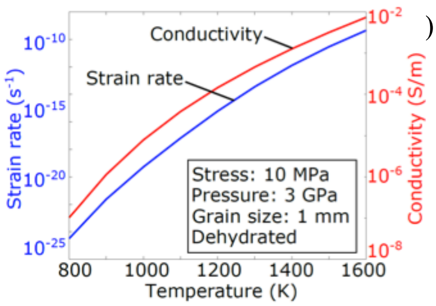

Figure 4. Both electrical conductivity (calculated from formulations in *Gardés et al.* [2014]) and strain rate (calculated from *Hirth and Kohlstedt* [2003] and *Ohuchi et al.* [2015]) are strongly sensitive to temperature. Calculations were made at 10 MPa stress, 3 MPa pressure and dehydrated conditions.

In the Archean to Proterozoic regions of southern and northern Greenland, the cold geotherms and geochemically depleted and dehydrated mantle compositions should lead to both high viscosities and high electrical resistivities. In contrast, beneath the Iceland plume track in central Greenland, the presumed hotter geotherm and hydration should lead to low viscosities and low electrical resistivities (see Fig. 7). By collecting and analysing MT data, we will test this model and constrain the Greenland mantle viscosity structure. In addition, by imaging conductive basal melt layers, we will test whether increased surface heat flow associated with the plume track is leading to increased melting of the ice sheet [e.g., *Rogozhina et al.*, 2016].

This ability to image temperature, hydrogen content and partial melt makes MT arguably the most important technique for constraining mantle viscosity. Seismic data, which are much more spatially extensive than MT data, are often used to build mantle viscosity models [e.g., *Kaufmann and Lambeck*, 2000; *Peltier et al.*, 2015]. Seismic velocities are temperature-dependent, so they should be related to viscosity. However, seismic velocity is also strongly affected by major element chemistry, which does not significantly impact viscosity. Conversely, viscosity is strongly affected by hydrogen content (Eq. 1), while seismic velocity is not. A direct conversion from seismic velocity to viscosity assumes that only temperature strongly affects seismic velocities and viscosities. MT data are strongly sensitive to hydrogen content, while also being sensitive to temperature and partial melt, and are therefore uniquely able to improve mantle viscosity calculations.

*2.5. **Hypothesis 2**: GIA models that include constrained viscosity variations will improve ice loss estimates*

Because Greenland is tectonically passive, vertical ground motion results from a combination of the elastic response to present-day melting (Fig. 2a) and the GIA response to past deglaciation (Fig. 2b). Vertical motions associated with mantle convection (dynamic topography) are thought to be >100 times slower [*Austermann et al.*, 2017]. Thus, observations of ground motion (e.g., GPS observations in Fig. 5) need to be accurately corrected only for GIA in order for these observations to be related to the patterns and rates of present-day melting [*Simpson et al.*, 2011], but this correction is significant. Indeed, we note several discrepancies between recent GPS uplift rates on the Greenland coastline and the uplift predicted by the combination of GIA from ICE-5G (Fig. 2b) and the elastic response to recent satellite-constrained melting (Fig. 2a) (see comparison in Fig. 5). In general, observed uplift rates are faster than predicted rates, especially along Greenland's south-eastern and western coasts. These discrepancies may be due to underestimation of uplift rates associated with either recent ice mass loss or GIA (that is, uplift in either Fig. 2a or Fig. 2b is too small). *Khan et al.* [2016] noted this trade-off, and suggested that most GIA models underestimate uplift rates because they do not account for the laterally-varying viscosity heterogeneity associated with the Iceland plume track. Furthermore, an accurate correction for GIA is essential for converting satellite observations (e.g., geoid changes from GRACE [*Harig & Simons*, 2016] or elevation changes from altimetry [*Hurkmans et al.*, 2014]) into mass loss rates [*Sutterley et al.*, 2014]. This project will specifically address this problem by providing improved GIA models that take into account new constraints on Greenland's 3D viscosity structure (from Hypothesis 1). These new GIA models will be immediately useful for interpreting geodetic constraints in terms of Greenland's recent melting history.

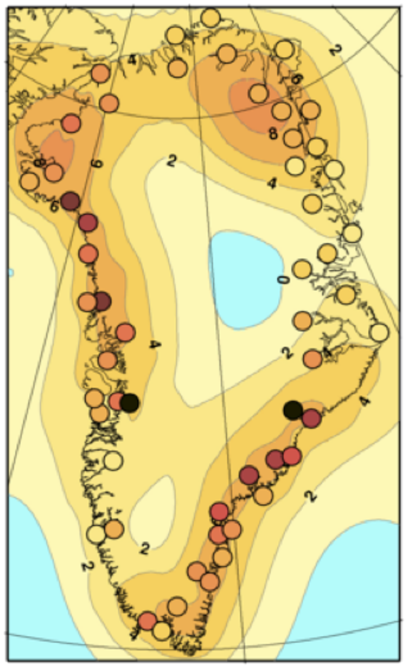

Figure 5. Comparison of uplift rates (colors) measured by GPS stations (circles, [*Khan et al.*, 2016]) and predicted by a model (background) that combines elastic uplift from present-day melting with GIA associated with ICE-5G deglaciation (that is, Fig 2a + 2b).

3. The project plan, project management, organisation and cooperation

The implementation of this project consists of four major work packages, which build upon each other:

	Work Package Description	**Lead**	**Participants**	**Period**
WP1	MT Data Collection on the Greenland Ice Sheet	KS	CC, PS, PhD, MA	2019–20
WP2	Viscosity structure from MT Modelling	KS, CC	KN, NK, PhD, MA	2019–20
WP3	GIA Modelling with Lateral Viscosity Variations	CC	LT, PS, MA	2019–21
WP4	Linking Modern Deglaciation to GIA & Geotherms	CC	All	2020–22

Research Group: CC = C. Conrad, KS= K. Selway, PS = Postdoctoral Scholar, PhD = PhD student, MA = Masters students
CG = C. Gaina, NK = N. Karlsson, KN = K. Nisancioglu, BS = B. Steinberger, LT = Lev Tarasov

*3.1 **Work Package WP1**: MT Data Collection on the Greenland Ice Sheet*

MT data are collected by deploying magnetometers and electric dipoles to log fluctuations in electric and magnetic fields. Each station consists of orthogonal electric dipoles, commonly 50–100 m long, and either a three-component fluxgate magnetometer (for a long-period station) or three orthogonal induction coil magnetometers (for a broadband station) to measure the magnetic fields in two orthogonal horizontal directions and vertically (Fig. 6). The length of recording time for a station determines the period range of the signal that can be recovered. For crustal-scale surveys, broadband stations may be deployed for as little as one day, whereas for lithospheric-scale surveys, long-period stations are deployed for up to several weeks.

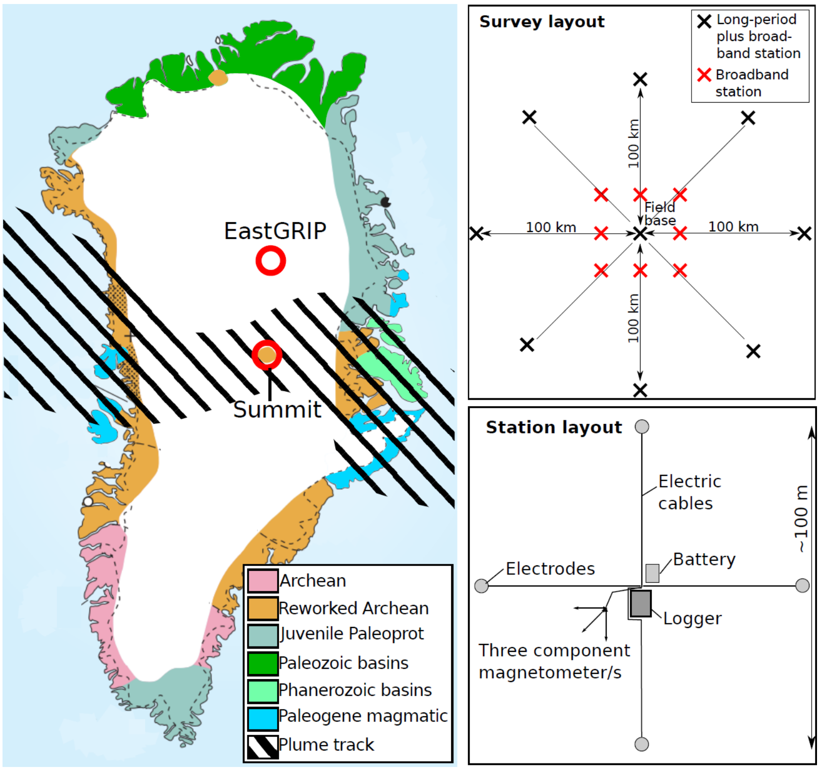

Figure 6. Map of Greenland showing the main geological demarcations (adapted from *Henriksen et al.* [2009]) and the reconstructed Iceland plume track [e.g., *Doubrovine et al.*, 2012]. One field season is planned for Summit Station, which lies over the Iceland plume track. The second is planned for EastGRIP station, which is away from the plume track. The hub and spoke survey design will allow three-dimensional models of the lithosphere to be produced. Long-period stations (black crosses) will be deployed for at least two weeks to resolve mantle features. Broadband stations (red crosses) will resolve crustal features and basal melt.

MT data collection can be complicated in polar regions by two factors. First, the extremely high electrical resistivity of snow and ice leads to high contact resistances between the Earth and the electrodes. However, this problem can be overcome by using pre-amps designed for polar conditions [*Wannamaker et al.*, 2004], with which Selway has significant experience. Second, the MT method assumes that the source field is a vertically propagating plane wave but proximity to the magnetic pole can lead to theoretical violations of this assumption. Previous experience in polar regions suggests that these 'source field effects' can sometimes be minor and can be corrected by removing data collected at times when the plane wave assumption is violated [*Peacock & Selway*, 2016; *Wannamaker et al.*, 2018; *Wannamaker et al.*, 2004]. We will test for source field effects by implementing the methods detailed in *Peacock & Selway* [2016] and by deploying grids of long-period stations to calculate inter-station magnetic transfer functions.

We will collect MT data in two field campaigns (Fig. 6). The first will be based out of the US National Science Foundation's 'Summit Station', which lies over the Iceland plume track in central Greenland. We have NSF approval that this project aligns with their science priorities at Summit and we will carry out a pilot survey there in mid-2018. The second will be based out of the 'EastGRIP' camp, which lies in north-eastern Greenland away from the Iceland plume track and is jointly funded by Denmark, USA, Germany, Norway, France, Japan and Switzerland. Nisancioglu is PI for EastGRIP camp in Norway. The surveys will be designed in a hub and spoke pattern, with a central long-period base station and additional long-period spoke stations deployed at radii of ~100 km (Fig. 6), allowing a 3D model of Earth electrical conductivity to be produced. In addition, broadband deployments, designed to resolve any basal melting of the ice cap, will be co-located with the long-period stations and additional stand-alone broadband stations will be deployed as densely as possible. Stations will be accessed by snow scooter and the instruments will be powered by batteries trickle-charged from solar panels. Long-period stations will record for at least two weeks in order to resolve mantle features and we estimate that each field season will last approximately six weeks to allow time for deployment and recording. MT instruments will be available from the Australian ANSIR pool.

*3.2 **Work Package WP2**: Constraining Greenland's Mantle Thermal and Viscosity Structure from MT*

MT data will be analysed using standard methods, including the multi-site, multi-frequency code of *Egbert* [1997] for processing and the phase tensor technique [*Caldwell et al.*, 2004] for determining dimensionality.

2D MT inversions will be primarily run with the MARE2DEM code [*Key*, 2016], which contains an adaptive mesh that will aid in defining sharp conductivity contrasts like the base of the ice and basal melt layers. Conductors at the base of the ice sheet that appear to represent basal melt will be interpreted in conjunction with radar data [e.g., *Fahnestock et al.*, 2001] with the assistance of collaborators Dr. Karlsson and Dr. Nisancioglu. 3D MT inversions will primarily be run using ModEM [*Kelbert et al.*, 2014]. All inverse models will be interrogated to test which features are robust and to determine resistivity ranges allowed by the data.

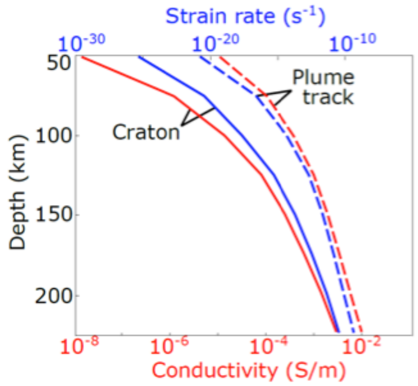

Figure 7. Hypothetical profiles of strain rate (blue) and conductivity (red) in the Greenland lithosphere both beneath the craton (solid lines) and the plume track (dashed lines). The craton has a typical, 40 mW/m^2 geotherm and a dehydrated composition; the plume track geotherm is elevated by 50 K and it contains 50 ppm hydrogen. These modest differences lead to conductivity contrasts of several orders of magnitude and strain rate contrasts that will affect GIA behaviour.

Mantle temperatures, hydrogen contents and partial melt contents will be calculated by combining the resistivity data with experimental mineral physics data [e.g., *Gardés et al.*, 2014; *Wang et al.*, 2006; *Yoshino et al.*, 2009], seismic data [e.g., *Lebedev et al.*, 2018] and surface heat flow, lithospheric thickness and xenolith data. There is inherent uncertainty in the interpretation of geophysical data since a number of physical properties may cause an observed anomaly. For instance, moderate conductivities may be caused by high hydrogen contents, slightly elevated temperatures, or other compositional effects. In contrast, some modelled conductivities may be too high to feasibly be caused by conduction in standard mantle minerals, suggesting either that melt is present (at high temperatures) or additional conductive minerals are present (at lower temperatures). We will decrease this uncertainty by utilizing xenolith constraints and jointly interpreting the MT data with existing seismic data. This joint interpretation will significantly tighten temperature constraints since both methods are affected by temperature but have different sensitivities to composition. We will quantify our interpretations using probabilistic approaches that incorporate uncertainties in resistivity, geotherm, and experimental conductivity. The calculated thermal, partial melt, and hydrogen content data will be combined to calculate constrained viscosities of the Greenland mantle (Eq. 1; Fig. 7).

*3.3 **Work Package WP3**: Postglacial Rebound (GIA) Modelling with Lateral Viscosity Variations*

We plan to develop improved GIA models that incorporate the new viscosity constraints from WP1 and WP2. For this, we need to build a GIA modelling technique that can accommodate lateral viscosity variations. We propose to do this using ASPECT [*Kronbichler et al.*, 2012], which is a parallelized, finite element code designed to solve for viscoelastic deformation in planetary mantles. This code is under active development by the Computational Infrastructure for Geodynamics (CIG), who provide it as open source software at https://geodynamics.org/cig/software/aspect/. Although this code has not been used previously to solve GIA problems, it has a major advantage over previous codes used for GIA as it uses adaptive mesh refinement (AMR), which automatically refines grid resolution in areas of rapid deformation while maintaining coarser resolution elsewhere, thus saving computational resources. We expect that large upper mantle viscosity variations beneath Greenland will localize deformation associated with the GIA response, and the AMR feature of ASPECT should enable us to resolve these finer-scale deformations at reduced computational cost.

ASPECT's functionality already includes essential features such as viscoelasticity, a free surface, and time-dependent forcing from surface tractions. For the GIA problem, self-gravitation must be implemented, which can be done as a post-processing step following *Zhong et al.* [2008]. We must also couple ASPECT to a solver for the sea level equation, which redistributes water loads based on the newly-deflected solid and ocean surfaces. We plan to implement a sea level solver within ASPECT, following the approach of SELEN [*Spada and Stocchi*, 2007] and adding rotational feedback and shoreline migration following *Paulson et al.* [2005]. SELEN is available from CIG (https://geodynamics.org/cig/software/selen/). We plan to work with the CIG center to implement this coupling and will make the new code available from CIG as open-source.

After we have developed and benchmarked our new GIA code, we will use it to solve the GIA problem for Greenland's laterally-varying viscosity structure. We will start by applying an ice history load based on the GLAC-1D model (https://pmip4.lsce.ipsl.fr/doku.php/data:ice_glac_1d), including updates currently being implemented by collaborator Tarasov. GLAC-1D [*Briggs et al.*, 2014; *Tarasov et al.*, 2012; *Tarasov and Peltier*, 2002] is based on a glaciological model constrained by a variety of geological [*Lecavalier et al.*, 2014] and present-day [*Briggs et al.*, 2014] constraints, and is therefore not linked to a specific GIA model or mantle viscosity structure. With Tarasov, we will implement the ice history into our new GIA code and examine possible variations to this history that lie within the uncertainty range. Output of WP3 will thus consist of a new open-source code that determines GIA deformation for a laterally-varying mantle viscosity structure, and new model predictions of GIA uplift for present-day Greenland.

*3.4 **Work Package WP4**: Updating Models of Present-Day Deglaciation with New Geotherms and GIA Data*

We will use the output of WP2 and WP3 to constrain rates and patterns of modern-day deglaciation for the Greenland Ice Sheet. WP2 will provide new, better-constrained geotherms that we will relate to mantle heat flow and melting at the base of the ice sheet. WP3 will produce new GIA models that we will use to constrain modern-day deglaciation rates. In WP4, we will convert these characterizations of Greenland's lithospheric structure and deformation rates into useful constraints on the critically important problem of the melting patterns and rates of the Greenland Ice Sheet. We anticipate contributions to this effort from all project leaders and collaborators. To facilitate this, we plan a joint seminar during the 3rd year of the project (2021) of all collaborators, relevant members of their research groups, and several invited outside experts. We will use this seminar to assess the discoveries of the MAGPIE project and to make plans to build upon them collaboratively in the final year of the project.

Surface heat flow is a fundamental parameter controlling basal melting of ice sheets, which in turn strongly impacts glacial flow and ice sheet stability [*Fahnestock et al.*, 2001]. Borehole measurements of surface heat flow exist at only a few locations on Greenland [*Rysgaard et al.*, 2018] so broader geotherms must be determined from geophysical data. With collaborators Selway, Steinberger and Gaina, we will use the improved mantle temperatures calculated in WP2 to construct new geotherms for Greenland. Through comparison between mantle geotherms and Curie depths, we will constrain both the mantle contribution and the crustal radiogenic contribution to surface heat flow beneath the ice sheet. We will therefore improve models for the thermal evolution of the Greenland mantle, including constraining plume impingement on the Greenland lithosphere. This effort will utilize plume flow models that have already been developed by Dr. Steinberger's group (e.g., for the Kerguelen hotspot [*Bredow and Steinberger*, 2018]) and will incorporate constraints from the tectonics and volcanism of the North Atlantic, with the assistance of Dr. Gaina [e.g., *Gaina et al.*, 2017].

Spatial patterns of basal melting of the Greenland Ice Sheet are currently determined largely through ice-penetrating radar data [e.g., *MacGregor et al.*, 2015]. Radar data suggest extensive basal melting beneath the North-East Greenland Ice Stream [e.g., *MacGregor et al.*, 2015; *Rogozhina et al.*, 2016], where borehole heat flow measurements are also anomalously high [*Rysgaard et al.*, 2018] and the NorthGRIP drillhole encountered basal melt [*Dahl-Jensen et al.*, 2017]. In contrast, neither radar nor drillhole data suggest the presence of basal melt beneath Summit Station [*Gow and Meese*, 2017], despite Summit lying over the reconstructed Iceland plume track (Fig. 6). *Rogozhina et al.* [2016] explained these discrepancies by suggesting that the plume track lies north of most reconstructions. Our survey locations at EastGRIP, where there is basal melt but no predicted plume track, and Summit, where reconstructions place the plume track but there is no basal melt, are ideally located to test these ideas. With collaborators Selway, Karlsson and Nisancioglu, we will combine our new geotherms from WP2 with existing radar and surface heat flow data to compare mantle temperatures with basal melting, constraining the geological controls on basal melting throughout Greenland. Conductors related to basal melt imaged in WP1 and WP2 will help to define the location and extent of melting. We will work with collaborator Tarasov to incorporate our new constraints on basal melting and geothermal heat flux into glaciological ice history models [e.g., *Briggs et al.*, 2014].

Our new GIA models produced in WP3 will allow us to develop improved constraints on patterns and rates of mass loss in Greenland during the past few decades. To achieve this, we will remove the GIA-induced vertical motions predicted by our models from GPS constraints on recent uplift (e.g., Fig. 5), most of which are continuous for the past decade [*Khan et al.*, 2016]. After accounting for GIA, the resulting uplift is caused by Earth's elastic response to on-going mass loss (e.g., Fig. 2a). Our new GIA model that incorporates lateral viscosity variations will thus significantly improve constraints on this melting. To utilize this new constraint, we will test a range of modern-day melting patterns (e.g., varying contributions from different drainage basins [*Andersen et al.*, 2015]) for their ability to reproduce the GIA-corrected GPS motions.

Other constraints on mass loss, such as those derived from temporal changes in ground-based [*Nielsen et al.*, 2014] or satellite [*Harig and Simons*, 2016; *Luthcke et al.*, 2013] gravity and from altimetry [*Hurkmans et al.*, 2014] are also highly dependent on the GIA model [*Sutterley et al.*, 2014]. We will re-visit these constraints using our new GIA models. Our ultimate objective is to use each these observational constraints, and combinations of them, to invert for the spatial patterns of recent mass loss, and to relate this loss to global sea level [*Frederikse et al.*, 2018] and its spatial variations [*Bamber and Riva*, 2010]. Essential to this goal are the new class of GIA models that we will develop (WP3) by incorporating viscosity constraints from Greenland fieldwork (WP1) and subsequent magnetotelluric analysis (WP2).

4. Key perspectives and compliance with strategic documents

Compliance with strategic documents. The project follows the vision of CEED as it enhances our understanding of Earth's interior dynamics and their interaction with Earth's surface environment.

Relevance and benefit to society. The Greenland Ice Sheet is a major contributor to recent sea level rise [*Frederikse et al.*, 2018], and its rate of melting is accelerating [*Harig and Simons*, 2016]. As this acceleration advances, it will become increasingly more important to use uplift observations to monitor Greenland mass loss and its contribution to global sea level rise. This project will provide new constraints on the 3D mantle viscosity structure and use them to constrain patterns and rates of uplift associated with Greenland's past history of deglaciation. This new postglacial rebound model for Greenland will provide a framework for evaluating present and future observations of uplift, and will therefore become a crucial element for constraining mass loss on the Greenland ice sheet, and the associated sea level change, in the coming century.

Environmental impact. MT is a passive method of geophysical observation and therefore the environmental impacts of this project are limited to travel and are minimal for the field sites on the Greenland ice sheet. By contrast, we expect that this project will help to characterize current and future ice melting rates in Greenland, which are a consequence of global climate change that directly impact global sea level.

Ethical perspectives. We anticipate no ethical conflicts, according to the ethics checklist provided.

Gender issues (Recruitment of women, gender balance and gender perspectives). Key project members K. Selway, C. Gaina and N. Karlsson are prominent female scientists and will serve as role models for the students involved in this project. We will prioritize female applicants for the student positions associated with this project, as scientific qualifications allow.

5. Dissemination and communication of results

We plan to actively publicize the results of our research by publishing in high-profile international journals and by presenting at international and regional conferences. We also plan an active public outreach campaign that includes public lectures, participation in science fairs (e.g., Forskningstorget), and articles in popular science forums. The Greenland fieldwork will be promoted in detail via blog posts and by coordination with science journalists via CEED's media contacts. Our outreach effort is detailed in the grant application form.

References

Andersen, M. L., et al. (2015), Basin-scale partitioing of GIS mass balance components (2007–11), *EPSL*, *409*, 89-95.

Aulbach, S., et al. (2018), Volatile-rich metasomatism in the cratonic mantle beneath SW Greenland: Link to kimberlites and mid-lithospheric discontinuities, *J. Petrology*, *1*, 28.

Austermann, J., et al. (2017), Detection of a dynamic topo sig. in the last interglacial sea-level record, *Science Advances*, *3*.

Bamber, J., and R. Riva (2010), The sea level fingerprint of recent ice mass fluxes, *The Cryosphere*, *4*, 621-627.

Bernstein, S., et al. (2006), Ultra-depleted, shallow cratonic mantle beneath West Greenland: dunite xenoliths from Ubekendt Ejland., *Con.. Min. Pet.*, *152*, 335.

Bernstein, S., et al. (1998), Depleted spinel harzburgite xenoliths in Tertiary dykes from East Greenland: restites from high degree melting, *Earth Planet. Sci. Lett.*, *154*, 221-235.

Bizzarro, M., & R.K. Stevenson (2003), Major element comp. of litho. mantle under the NAC:Evidence from peridotite xenoliths of the Sarfartoq area, SW G.land, *Cont.. Min. Pet.*, *146*, 223-40.

Bredow, E., & B. Steinberger (2018), Variable melt production rate of the Kerguelen hotspot due to long-term plume-ridge interaction, *Geophys. Res. Lett.*, *45*, 126-136.

Briggs, R.D., et al. (2014), A data-constrained large ensemble analysis of Ant. evltion. since Eemian, *Q. Sci. Rev.*, *103*, 91-115.

Caldwell, T.G., et al. (2004), The magnetotelluric phase tensor, *Geophys. J. Int.*, *158*, 457-469.

Conrad, C. P. (2013), The solid Earth's influence on sea level, *Geol. Soc. Am. Bullet.*, *125*, 1027-1052.

Dahl-Jensen, et al. (2017), Basal melt at NorthGRIP modeled from borehole, ice-core & radio-echo sounder observations., *An. Glac.*, *37*, 207-12.

de Boer, B., et al. (2017), Current state and future persp. on coupled ice-sheet – sea-lev. mod., *Qua. Sci. Rev.*, *169*, 13-28.

Doubrovine, P.V., et al., (2012), Absolute plate motion in reference frame defined by moving hotspots in the Pacific, Atlantic, & Indian oceans., *JGR*, *117*, B09101.

Egbert, G. D. (1997), Robust multiple station magnetotelluric data processing, *Geophys. J. Int.*, *130*, 475-496.

Fahnestock, M., et al. (2001), High geot. heat flow, basal melt, and orig. of rapid ice flow in cent. G.land, *Sci.*, *294*, 2338-42.

Frederikse, T., et al. (2018), A constrained sea-level reconstruction & its budget on basin and global scales over 1958–2014, *J. Clim.*, *3*, 1267-1280.

Gaina, C., et al. (2017), Break-up and seafloor spreading domains in the NE Atlantic, *Geol. Soc. Lond. Spec. Pub., 447*, 393-417.

Gardés, E., et al. (2014), Toward a unified hydrous olivine electrical conductivity law, *Geochem., Geophys., Geosys., 15*, 4984-5000.

Gow, A. J., and D. A. Meese (2017), Nature of basal debris in GISP2 and Byrd ice cores & its relevance to bed processes, *Ann. Glac.*, *22*, 134-40.

Griffin, W., et al. (2009), The composition and evolution of lithospheric mantle: a re-evaluation and its tectonic implications, *J. Pet.*, *50*, 1185-1204.

Harig, C., and F. J. Simons (2016), Ice mass loss in Greenland, the Gulf of Alaska, and the Canadian Archipelago: Seasonal cycles and decadal trends, *GRL*, *43*, 3150-3159.
Henriksen, N., et al. (2009), Greenland from Archaean to Quaternary. Descriptive text to the 1995 geological map of Greenland, 1:2 500 000 edition, GEUS, vol 18.
Hirth, G., & D. Kohlstedt (2003), Rheology of the upper mantle & the mantle wedge: A view from the experimentalists, *Inside the subduction factory*, 83-105.
Hurkmans, R.T.W.L., et al. (2014), Time-evolving mass loss of the Greenland Ice Sheet from satellite altimetry, *The Cryo.*, *8*, 1725-40..
Kaufmann, G., & K. Lambeck (2000), Mantle dynamics, postglacial rebound and the radial viscosity profile., *PEPI, 121*, 301-324.
Kelbert, A., et al. (2014), ModEM: A modular system for inv. of electromagnetic geophys. data, *Comp. Geosci.*, *66*, 40-53.
Key, K. (2016), MARE2DEM: A 2-D inv. code for controlled-source eletromag. and MT data, *Geophy. J. Int.*, *207*, 571-588.
Khan, S. A., et al. (2016), Geodetic measurements reveal similarities between post–LGM and present-day mass loss from the Greenland ice sheet, *Sci. Adv.*, *2*,.
Khan, S.A., et al. (2010), Spread of ice mass loss to NW G.land obs. by GRACE & GPS, *GRL*, *37*, L06501.
Kronbichler, M., et al. (2012), High accuracy mantle convection simulated through modern numerical methods, *Geophys. J. Int.*, *191*, 12-29.
Latychev, K., et al. (2005), GIA on 3-D Earth models: a finite-volume formulation, *Geophys. J. Int.*, *161*, 421-444.
Lebedev, S., et al. (2018), Seismic tomography of the Arctic region: inferences for the thermal structure and evolution of the lithosphere, *Geol. Soc., Lond., Spec. Pub.*, *460*, 419-440.
Lecavalier, B. S., et al. (2014), A model of Greenland ice sheet deglaciation constrained by observations of relative sea level & ice extent, *Quat. Sci. Rev.*, *102*, 54-84.
Liu, L., and D. Hasterok (2016), High-res lithosphere viscosity and dynamics revealed by MT imaging, *Sci.*, *353*, 1515-19.
Luthcke, S.B., et al. (2013), Antarctica, Greenland & Gulf of Alaska land-ice evolution from iterated GRACE global mascon solution, *J. Glac.*, *59*, 613-31.
MacGregor, J. A., et al. (2015), Radiostratigraphy and age structure of the Greenland Ice Sheet, *JGR, 120*, 983-1008.
Mitrovica, J. X., et al. (1994), A spectral formal. for computing 3D deform. due to surf. loads, *J. Geophys. Res.*,, *99*, 7057-73.
Nichols, A., et al. (2002), Is the Iceland hot spot also wet? Evidence from the water contents of undegassed submarine and subglacial pillow basalts, *EPSL*, *202*, 77-87.
Nielsen, J. E., R. Forsberg, and G. Strykowski (2014), Measured & modelled absolute gravity changes in Greenland, *J. of Geody.*, *73*, 53-59.
Nutman, A. P., et al. (2008), Palaeoproterozoic and Archaean gneiss complexes in N. Greenland: Palaeoproterozoic terrane assembly in the High Arctic, *Precamb. Res.*, *161*, 419-451.
Nutman, A. P., et al. (1999), U–Pb zircon ages of Kangamiut dykes and detrital zircons in metasedents in the Paleoprot. Nagssugtoqidian Orogen (W. Greenland): Clues to the pre-collissional history of the orogen, *Precamb. Res. 93*, 87-104.
Ohuchi, T., et al. (2015), Dislocation-accomodated grain boundary sliding as the major deformation mechanism of olivine in Earth's upper mantle, *Sci. Adv.*, *1*, e1500360.
Paulson, A., S. J. Zhong, and J. Wahr (2005), Modelling post-glacial rebound with lateral viscosity variations, *Geophy. J. Int.*, *163*, 357-371.
Peacock, J. R., and K. Selway (2016), MT investigation of the Vestfold Hills and Rauer Group, East Antarctica, *JGR*, *121*, 2258-2273.
Peltier, W. R. (2004), Global glacial isostasy and the surface of the ice-age earth: The ICE-5G (VM2) model and GRACE, *Ann. Rev. Earth Planet. Sci.*, *32*, 111-149.
Peltier, W. R., D. F. Argus, and R. Drummond (2015), Space geodesy constrains ice age terminal deglaciation: The global ICE-6G_C (VM5a) model, *J. Geophys Res.*, *120*, 450-487.
Putirka, K. D. (2005), Mantle potential temperatures at Hawaii, Iceland, and the mid-ocean ridge system, as inferred from olivine phenocrysts: Evidence for thermally driven mantle plumes, *Geochemistry, Geophysics, Geosystems*, *6*(5).
Rogozhina, I., et al. (2016), Melting at the base of the Greenland ice sheet explained by Iceland hotspot history, *Nat. Geosci.*, *9*, 366-69.
Rysgaard, S., et al. (2018), High geothermal heat flux in close proximity to the NE Greenland Ice Stream, *Sci. Rep.*, *8*, 1344.
Schaeffer, A.J., & S. Lebedev (2013), Global shear speed struct. of the UM and trans. zone, *Geop. J. Int.*, *194*, 417-449..
Selway, K. (2015), Negligible effect of hydrogen content on plate strength in East Africa, *Nat. Geosci.*, *8*, 543.
Sifré, D., et al. (2014), Electrical conductivity during incipient melting in the oceanic low-velocity zone, *Nature*, *509*, 81.
Simpson, M.J.R., et al. (2011), The influence of decadal- to millennial-scale ice mass changes on present-day vertical land motion in Greenland: Implications for the interpretation of GPS observations, *J. Geophys Res.*,, *116*, B02406.
Spada, G., and P. Stocchi (2007), SELEN: A Fortran 90 prog. for solving the "sea-level eq.", *Comp. & Geosci.*, *33*, 538-562.
Steinberger, B., et al. (2015), The key role of global solid-Earth processes in preconditioning Greenland's glaciation since the Pliocene., *Ter. Nova*, *27*, 1-8.
Storey, M., et al. (1998), ^{40}Ar/^{39}Ar geochron. of the W. Grland Tertiary volc. province, *Earth Planet. Sci. Lett.*, *160*, 569-86.
Sutterley, T. C., et al. (2014), Evaluating Greenland glacial isostatic adjustment corrections using GRACE, altimetry and surface mass balance data, *Env. Res. Lett.*, *9*, 014004.
Tarasov, L., et al. (2012), A data-calibrated distribution of deglacial chronologies for the North American ice complex from glac. modeling, *Earth Planet. Sci. Lett.*, *315-316*, 30-40..
Tarasov, L., & W.R. Peltier (2002), Greenland glacial history and local geodynamic conseq, *Geophys. J. Int.*, *150*, 198-229.
Tegner, C., et al. (2008), ^{40}Ar–^{39}Ar ages of intrusions in East Greenland: Rift-to-drift transition over the Iceland hotspot, *Lithos*, *101*, 480-500.
van der Wal, et al. (2015), Effect of GIA models with 3D composite mantle viscosity on GRACE mass balance estimates for Antarctica, *EPSL*, *414*, 134-143.
Velicogna, I. (2009), Increasing rates of ice mass loss from G.land & Ant. ice sheets rev. by GRACE, *GRL*, *36*, L19503.
Wake, L.M., et al. (2016), Glacial Isostatic Adjustment (GIA) in Greenland: a Review, *Curr. Clim. Ch. Rep.*, *2*(3), 101-111.
Wang, D., et al. (2006), The effect of water on the electrical conductivity of olivine, *Nature*, *443*, 977.
Wannamaker, P., et al. (2018), Uplift of the central transantarctic mountains *Nature Comm.*, *9*. 1588.
Wannamaker, P. E., et al. (2004), Structure and thermal regime beneath the South Pole region, East Antarctica, from MT measurements, *Geo. J. Int.*, *157*, 36-54.
Weis, D., et al. (1997), Ice sheet development in central Greenland: implications from the Nd, Sr and Pb isotopic composition of basal material, *EPSL, 150*, 161-169.
Whitehouse, P., et al. (2006), Impact of 3-D Earth structure on Fennoscandia GIA: Imp. for space-geodetic estimates of present-day crustal deformations, *Geophys. Res. Lett.*, *3*, L13502.
Windley, B.F., & A.A. Garde (2009), Arc-gen. blocks with crustal sect. in N. Atl. craton of W. Greenland: crustal growth in the Archean with modern anal., *Earth-Sci. Rev.*, *93*, 1-30.
Yoshino, T., et al. (2009), The effect of water on the electrical conductivity of olivine aggregates and its implications for the electrical structure of the upper mantle, *EPSL.*, *288*, 291-300.
Zhong, S. J., et al. (2008), A benchmark study on mantle convection in a 3D spherical shell using CitcomS, *Geochem. Geophys. Geosys*. *9*, Q10017.